Civil and Environmental Engineering
Vol. 21, Issue 1, 383-392, DOI: 10.2478/cee-2025-0030

EVALUATION OF ULTIMATE BEARING CAPACITY AND INFLUENCE ZONE OF CLAY USING FEM: A COMPARISON WITH THEORETICAL MODELS

Rabab JABAR[1, *], Ressol R. SHAKIR[1]

[1] Civil Engineering Department/ University of Thi-Qar, Nasiriyah, Iraq.
corresponding author: rrshakir@utq.edu.iq

Abstract

This research aims to evaluate the ultimate bearing capacity of soft clay soil and indicate the form of the failure surface and the influence zone under a square foundation by utilizing the finite element method. A square foundation resting on a layer of clayey soil has been studied. The engineering characteristics of the clay soil have been retrieved from site investigation reports for the school project executed in Naseriyah. Seven groups of data have been used for seven cases of projects with a range of undrained cohesion of about 31 to 51 kPa. The clay soil was modeled as a Mohr-Coulomb in the finite element analysis and subjected to a uniform distributed load at the center of the studied area. The dimensions of the soil under the foundation have been selected so that the stresses at the boundary vanishes. The results of finite elements were compared with five theoretical equations Prandtl's, Terzaghi’s, Meyerhof's, Hansen and Vesic's. It is concluded that (a) the results of finite element agreed with results obtained by Meyrhof equation and the error percent was 7%, then Hansen and Vesic with a percent of 8% while Terzaghi and Prandtle were not agreed with a percent of about 15%. (b) The dimensions of boundaries of the failure surface beneath a rigid strip footing submit to a centric vertical load and the depth ofthe failure zone is approximately equal to 1.15B.

Keywords:

Bearing Capacity 1;
FEM 2:
Influence Zone;
Soft Clay.

1 Introduction

Shallow foundations are subsurface structural members that transmit the structural load such as the loads arises from the low-rise buildings, to the soil [1],[2]. Understanding the soil's load-bearing capacity and its behavior is crucial to avoid shear failure, which occurs when the soil cannot support the applied stress, potentially leading to structural collapse [3]. The bearing capacity of soils depends mainly on the failure surface which in turn depends on the soil type and its density. As the boundary of the influence zone is modified the bearing capacity of soil is changed. Therefore, the failure surface gains a high interesting in computing accurate values of bearing capacity. The failure surface is assumed when theoretical derivation is selected while it is post-identified through numerical solution such as finite element solution.

Analytical and numerical methods are used to determine the bearing capacity in addition to the indicating of the failure surface. With respect to the analytical solution, researchers like Prandtl (1920) [4],Terzaghi (1943) [5],[6],[7] Meyerhof (1963) [8][9], Hansen (1970) [10],[11],[12], Vesic (1975) [13] have developed methods for calculating the ultimate bearing capacity of shallow foundations [14]. These methods requires assuming the failure surface before the derivation of the bearing capacity factors. However, modern numerical methods, such as finite element (FE) provide more accurate insights into complex soil behaviors and conditions, and influence zone can then be identified according to the stress intensity distribution [15],[16]. Numerical modeling, particularly the finite element method (FEM), is crucial in geotechnical engineering, enabling precise simulation of soil behavior and interactions with structures[17],[18]. Shakir, (2005)[19] advanced a software FEM use to determine the bearing capacity of a continuous foundation on undrained clay with one and two layers soil. The finite element solution can give a mesh deformation below the foundation and the distribution of stresses in addition to the deformation for different localized regions in the soil surrounding and supporting the footing.

Michalowski and Shi (2003) [20] observed that heave formation around strip footings on sandy soil often lacks symmetry at the point of failure, with the displacement patterns differing between loose and dense sand deposits. These findings suggest that the failure mechanisms in sandy soils deviate from the traditionally accepted symmetrical models, pointing to a more complex process. Given these contradictions, numerical evaluations focusing on the evolution of failure mechanisms rather than solely estimating bearing capacity are crucial. The mechanism of the failure in clay soil may also be similarly investigated using finite element method but with different mode of failure based on the consistency of the soil. Despite extensive research on bearing capacity, few studies have investigated the development and progression of failure mechanisms under gradually applied loads, highlighting a gap in current geotechnical studies.

The research focuses on analyzing the ultimate bearing capacity of soft clayey soils beneath square foundations using finite element methods, specifically through the application of Plaxis software. The primary goal is to validate the finite element approach by comparing its numerical results with traditional theoretical models. Additionally, the study aims to define the actual boundaries of the failure zones under foundations based on numerical analysis and compare these boundaries to those predicted by theoretical models. By doing so, the research seeks to provide a clearer understanding of the behavior of soil under loading conditions, and to assess the accuracy of finite element analysis in predicting failure zones in soft clay soils. Confirmation to the boundary dimensions can be achieved based on FE.

2 Geology of the study area

Geologically speaking, the structure of the soil located in the south of Iraq (such as at Nasiriyah) is the Mesopotamian plain, which dates back to the Pleistocene and Holocene periods[21],[22]. Alluvial silt deposits from the Tigris and Euphrates rivers can be found in this soil [23]. Because there has been no erosion of the ancient rock surface, Nasiriyah is located in a floodplain zone that reflects the recent surface creation of Iraq's geology [24]. The main components of these deposits include clay and silty clay, as well as soft layers of fine sand and silt. These strata can be found throughout this city, including the area under investigation.

3 Methodology

3.1 Preparation of data

The collected data was retrieved from the site investigation reports on seven distinct locations inside the region of Nasiriyah. The overall layout of the sites in Nasiriyah is presented in the Google image shown in (Fig. 1). Eslah, Tar, Shawalesh, Karmashya, Haboby, Neser, and Said-Dikiel are the locations of the projects under this study. All these projects are one and two story schools which represent a low rise building. (Fig. 1) depicts the site of the boreholes drilled through performing the soil subsurface exploration of these projects.

Fig. 1: Projects locations in the Nasiriyah city.

The data for this study were sourced from soil survey reports from various project sites in the southern part of Nasiriyah. These reports were gathered through site investigations conducted by different laboratory testing agencies. The soil properties used in this analysis are certified in the project-specific reports. (Fig. 2) shows sample of the stratigraphy of soil layers at borehole locations across four distinct sites, providing detailed insights into the subsurface conditions.

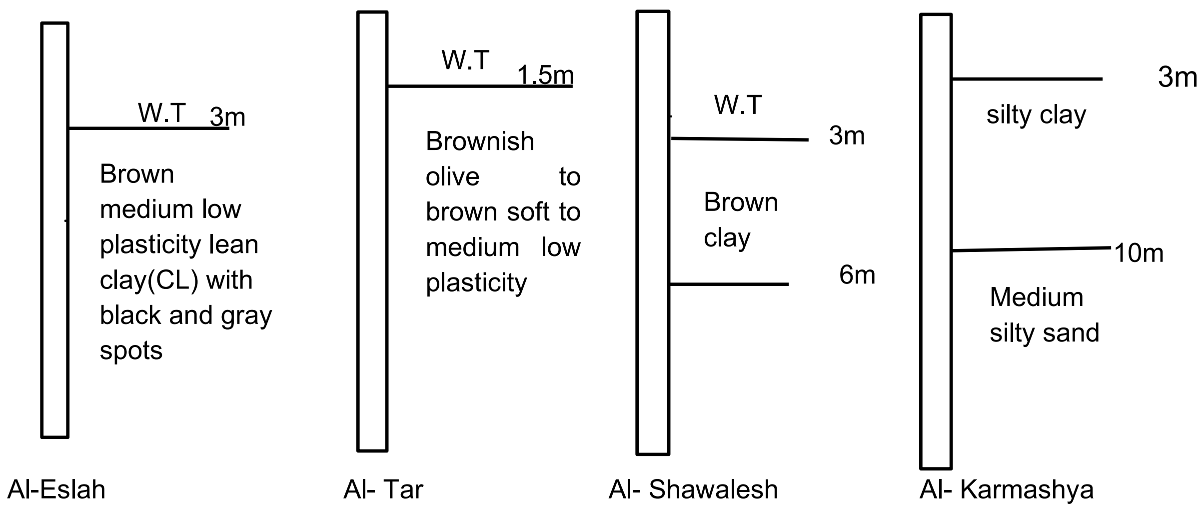

Fig. 2: Profile of the soil data.

Laboratory tests are conducted on the most disturbed and undisturbed samples delivered to the laboratory, including visual classification, liquid and plastic limits, specific gravity, unconfirmed compression, and standard penetration tests. The soil was classified visually and analyzed by grain size, and the results showed that it was mostly made up of one type of soil: a layer of brown medium-low plasticity lean. Table1 shows the parameters of clay soils obtained from the project reports and includes the modulus of elasticity, cohesion, and unit weight of soil. The modulus of elasticity of the soil was calculated based on the soil cohesion according to the equation[22] $E = 1200\, c_u$, where c_u is the undrained cohesion. The consistency of the soil at the site of the projects except the Haboby site is soft to medium since the unconfined compression was between 50 and 92 kN/m^2. At Haboby location the strength of the soil is considered as stiff soil.

Table 1: Soil Properties at the seven location of the projects.

No	Project area	BH	c [kN/m^2]	γ_{sat} [kN/m^3]	γ_d [kN/m^3]	v	Es [Mpa]
1	Eslah	BH1	34	19.35	18.52	0.35	40800
2	Tar	BH1	38	19.54	15.72	0.3	45600
3	Shawalesh	BH1	44	19.88	15.35	0.3	52800
4	Karmashya	BH3	25	20.21	16.63	0.35	29400
5	Habobey	BH2	52	20.26	16.22	0.4	61992
6	Neser	BH3	31	19.39	14.9	0.27	37440
7	Said Dikiel	BH3	46	19.1	18.74	0.26	55200

Definition of abbreviations

BH - Borehole,
c - Cohesion [kN/m^2],
γ *sat* - Saturated unit weight [kN/m^3],
γ*dry* - Dry unit weight [kN/m^3],
v - Poisson Ratio,
E - Modulus of Elasticity [Mpa].

3.2 Numerical Modelling

The finite element technique was used to study the load-settlement behavior of a square foundation with dimensions of (B=2 m), under the action of a vertical and stable load on clay soil using the commercial software PLAXIS 3D. Numerical analysis was performed under controlled conditions to simulate the behavior of the soil in situ accurately[25],[26],[27],[28]. The Mohr-Coulomb model, a popular model used to estimate the behavior of clay soils under moderate stiffness conditions, was used in this research. The model assumes a linear elastic-plastic behavior of the soil, which simplifies the analysis while providing reasonable accuracy. The model consists of a set of key parameters including cohesion (c), angle of internal friction (φ), modulus of elasticity (E), and Poisson's ratio (v), which together accurately describe the response of the soil under loading conditions [29][30]. This model provides accurate estimates of deformation with faster calculation times compared to more complex models such as the stiff soil model, although it may not capture the full nonlinear behavior of stress and strain under complex loading conditions. The soil model was designed with dimensions of at least 3B horizontally from the edge of the foundation and the same depth vertically towards the bottom boundary, to ensure that the effect of boundaries is minimized. The foundation was represented as a rigid structure with uniform stress distribution on its base, and appropriate boundaries were applied to simulate the realistic behavior of the soil. The lower boundary of the model was fixed to prevent displacements in all directions while sliding lateral boundaries were applied to allow vertical displacements while restricting. The finite element mesh was created with a clear refinement near the center of the foundation to capture the large changes in stresses and deformations that occur under and around the foundation Fig (3). As the distance from the foundation edge increased, a medium-sized mesh was used to balance computational efficiency and accuracy. The mesh refinement was based on convergence studies to ensure that the results are not affected by further mesh refinement, achieving a balance between computational efficiency and accuracy. However, using a very fine mesh increases computation time without significantly improving accuracy, especially in areas far from the foundation. The purpose of optimizing the grid near the foundation is to ensure accurate simulation of large stress-strain changes directly below the loaded area. As the distance increases, the effect of stress redistribution decreases, justifying the use of coarser grids to save computational resources while maintaining acceptable accuracy. The designed model is able to capture the fundamental aspects of foundation-soil interaction and provides reliable results for load-settlement predictions under realistic conditions.

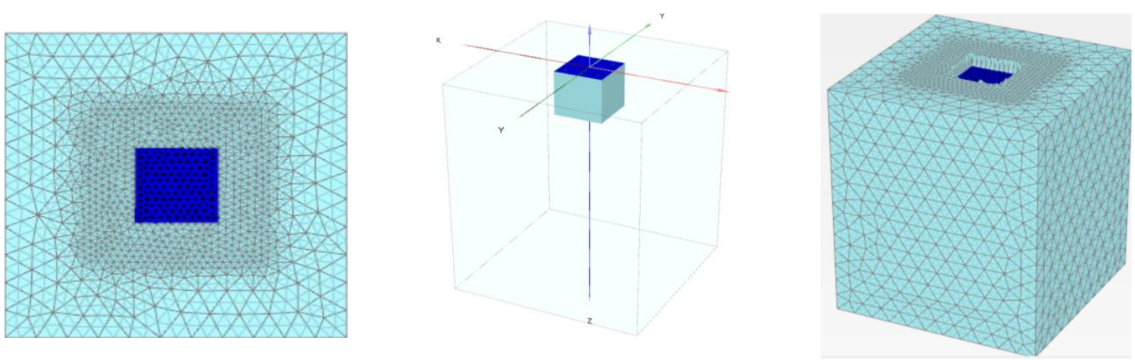

Fig. 3: Mesh of square footing resting on clay soil.

Table 2 lists several properties of the foundation, such as concrete density, elastic modulus (E), and poisons ratio, which are required as input for the Plaxis3D and program during the model's simulation.

Table 2: The foundation's parameters [31].

Shape	Dimension	Thickness [m]	Density γ [kN/m^3]	modulus elasticity E, [kN/m^2]	Poisson's Ratio.	Material Model
Square	2.0 x 2.0	0.4	24	3x107	0.2	Linear elastic

3.3 Verification of the FEM

To verify the solution by finite elements, a comparison will be made with the theoretical equations presented in the Table 3 [32]. In this Table, the design equations of five theoretical models are presented. These equations represent a wide range of most interesting equations used in the design of the shallow foundation. These methods, including Prandtl, Terzaghi, Meyerhof, Hansen, and Vesic, were specifically chosen because they are widely recognized and extensively used in geotechnical engineering. They provide a reliable foundation for comparing with numerical analysis results and allow for a comprehensive evaluation of the finite element method's accuracy. Moreover, these equations cover a variety of assumptions regarding soil behavior and failure mechanisms, making them suitable benchmarks for validating the FEM approach.

The following sections presents the comparison results and the boundary indication of the failure surface based both on numerical and analytical solution results obtained

Table 3: Theoretical equations used in calculating the bearing capacity of soil.

Method	Theoretical equations
Prandtl 1920	$q_u = cN_C + qN_q + \frac{1}{2}\gamma N_\gamma$
Terzaghi 1943	$q_u = 1.3cN_c + qN_q + 0.4\gamma BN_\gamma$
Meyerhof (1963)	$q_u = cN_cF_{cs}F_{cd}F_{ci} + qN_qF_{qs}F_{qd}F_{qi} + \frac{1}{2}\gamma BN_\gamma F_{\gamma s}F_{\gamma d}F_{\gamma i}$
Hansen (1970)	$q_u = cN_cS_cd_ci_c + qN_qS_qd_qi_q + 0.5\gamma BN_\gamma S_\gamma d_\gamma i_\gamma$
Vesic (1973)	$q_u = cN_cS_cd_ci_c + qN_qS_qd_qi_q + 0.5\gamma BN_\gamma S_\gamma d_\gamma i_\gamma$

4 Result and Discussion

4.1 Comparison between FE and theoretical solution of BC

To verify the validity of the finite elements solution specified in this research, the bearing capacity of clay soil solved by the finite element method was compared with the five ways shown in Table 3.

Table 4 shows the bearing capacity values based on different analytical solution besides the finite element solution. It is obvious that the bearing capacity values of the soil under the square foundation computed by the Prandtl equation are lower than values determined by other methods, including the FE solution. This indicates that they are more conservative or less sensitive to soil properties. The BC values obtained by the Terzaghi equation are higher than those obtained by the Prandtl method, but they are still lower than the results of FE. The BC computed based on the Meyerhof equation showed good agreement with the results calculated by FE, with relative differences of 6%, 1%, and 5% for the regions of Karmashya, Neser, and Eslah, respectively, as shown in Table 4. With respect to the BC values obtained by the method of Hansen and Vesic are very close, both are very close to Meyerhof values. Modern models like Vesic account for local shear failure processes. The lower error percentages suggest that the Meyerhof method approximates numerical analysis better.

Table 4: Comparison of ultimate bearing capacities for various regions using numerical analysis and theoretical methods.

NO	Region	FE solution (1)	Prandtl (2)	Terzaghi (3)	Meyerhof (4)	Hansen (5)	Vesic (6)
		ultimate bearing capacitie qu [kN/m^2]					
1	Karmashya	21.3	15.88	22.3	19.9	19.82	20.11
2	Neser	25.5	20.2	28.4	25.2	25.19	25.46
3	Eslah	25.9	22	30.9	27.4	27.4	27.8
4	Tar	28.0	24.6	34.6	30.7	30.9	31.1
5	Shawalesh	32.5	28.5	40.0	35.5	35.9	35.7
6	Said Dikiel	33.4	29.8	41.89	37.23	37.13	37.86
7	Habobey	47.14	33.5	46.99	41.75	41.67	41.96

The results, shown in Table 5, were analyzed using relative error to quantify the differences between theoretical predictions and finite element. In our analysis, the Meyerhof theory demonstrated the lowest error rate of 7%, indicating a good agreement with the results from the finite element analysis. This suggests that Meyerhof's assumptions and modifications are closely aligned with the approximate behavior of the clay soil model in the finite element method (FEM). Following this, the Hansen and Vesic equations showed slightly higher error rates of 8%, indicating a fairly good match with the FEM results but with some discrepancies likely due to differences in their bearing capacity formulations. On the other hand, the Prandtl and Terzaghi equations exhibited a significantly higher error rate of 15%, suggesting that these models deviate more from the FE results and may not capture the soil's response as accurately under the given conditions.

Table 5: Quantitative evaluation of results using relative error.

NO	Region	Relative error [%] Prandtl	Relative error [%] Terzaghi	Relative error [%] Meyerhof	Relative error [%] Hansen	Relative error [%] Vesic
1	Karmashya	25.44601	4.694836	6.57277	6.948357	5.586854
2	Neser	20.78431	11.37255	1.176471	1.215686	0.156863
3	Eslah	15.05792	19.30502	5.791506	5.791506	7.335907
4	Tar	12.14286	23.57143	9.642857	10.35714	11.07143
5	Shawalesh	12.30769	23.07692	9.230769	10.46154	9.846154
6	Said Dikiel	10.77844	25.41916	11.46707	11.16766	13.35329
7	Habobey	28.93509	0.318201	11.43403	11.60373	10.98854
	Average	17.92176	15.39402	7.902209	8.220804	8.334149

(Fig. 5) shows a comparison of bearing capacity for different regions. The x-axis represents different calculation methods, and the y-axis represents the bearing capacity values for each region. The Haboby area displays consistently higher bearing capacity while the Karmashya area shows lower bearing capacity due to the difference in soil cohesion, moisture content, and compaction levels on these bearing capacity values. The bearing capacity for soil in Haboby region was relatively high due to stronger soil properties.

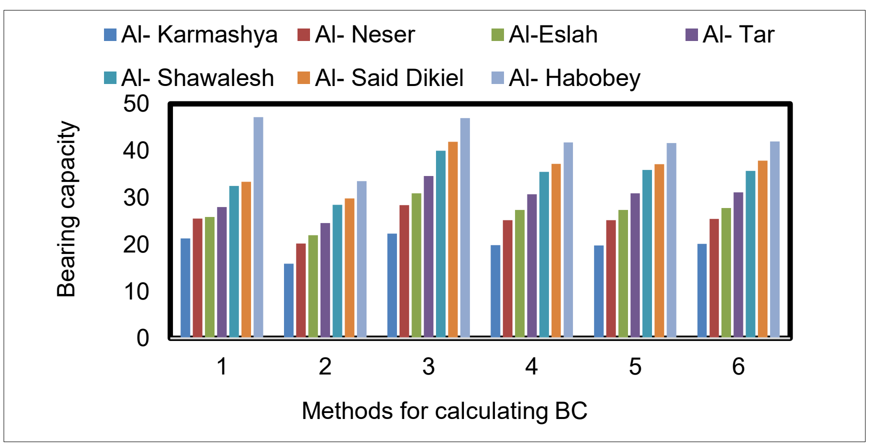

Fig. 5: Comparison of bearing capacity values for different regions.

The analysis demonstrates that the finite element method (FE) offers precise insight into the behavior of clay soils under loads. For instance, FE results align closely with the Meyerhof method, Particularly in regions such as Karmashya and Neser, where the error percentage was less than 6% This indicates that numerical modeling can predict the bearing capacity more realistically compared to traditional theoretical models. On the other hand, the Prandtl and Terzaghi methods yield more conservative results, with differences reaching up to 25%, suggesting that these methods may underestimate the actual bearing capacity of soils in certain cases. Table 4 provides a comprehensive comparison of all methods, highlighting the performance differences among the various models.

4.2 Influence zones

Terzaghi's equations were used to calculate the boundaries of the influence zones in the case of the Haboby area, and the results showed that applying these equations to other cases gives close values. In contrast, the solution using Meyerhof's equations was close to the results obtained by using Terzagi's method in determining the failure zones. Hansen's equations dealt with soil failure from the perspective of maximum stresses. The influence zones were also determined using finite elements. Here are the Terzaghi's equations for calculating the failure zones:

1. Zone I is essentially the elastic region beneath the footing. Its size is typically taken as the width of the footing and extends vertically downward a distance approximately equal to the depth of the footing.

2. Zone II (Radial Shear Zone) Zone II is the region where radial shear occurs. The slip lines in Zone II fan out from the edges of Zone I by the soil's angle of internal friction. The equation for the boundary of Zone II:

$r = R_o e^{\theta tan\varphi}$

r = radial distance from the edge of the footing

R_O = radius of the elastic zone (taken as half the width of the footing, ($B/_2$)

θ = angle measured from the vertical axis at the edge of the footing

φ = angle of internal friction

3. Zone III is the passive failure wedge the boundary of Zone III can be approximated by the failure wedge extending from Zone II at an angle α

$$\alpha = 45 + \frac{\varphi}{2}$$

The equation for the boundary of Zone III:

$$L = B + 2Htan(45 + \frac{\varphi}{2})$$

L = The horizontal extent of Zone III

B = width of the footing

H = depth of the footing

Table 6 shows the values of the influence zone boundaries according to Terzaghi's equations and the Plaxis analysis. Terzaghi predicts an elastic influence zone directly below the foundation of about 0.5 m equal to the depth of the foundation, while the Plaxis analysis shows a larger value of 0.971 m. This indicates that the numerical analysis captures a wider elastic zone, perhaps due to more consideration of the soil stiffness or properties in the finite element model.

Region II is estimated by Terzaghi to be 1m, but the FE method estimates 1.934 m, which means that the radial shear region in the real soil model captured by FE method extends beyond that, which is not explained by Terzaghi's simplified approach.

With respect to Region III, Terzaghi estimates this region to be the widest at 3m, while FE method presents a smaller impact region of 2.3 m. This suggests that the Terzaghi model may overestimate the negative region while Plaxis estimates a more conservative estimate based on local failure mechanisms.

Table 6: Comparison of influence zone boundaries between Terzaghi's theory and FEanalysis.

Method	**Influence zones(m)**		
	Zone I	**Zone II**	**Zone III**
Terzaghi	0.5	1	3
FE analysis	0.971	1.934	2.3

(Fig. 6) shows the application of the finite elements to the clay soil of the Habobey area, where the soil cohesion is measured at 51kN/m2. Therefore the more cohesive soil found in the Al-Haboubi area was selected as an example. This area represents a type of soil with superior properties in terms of cohesion and resistance to failure, making it more suitable for supporting structural loads without undergoing the same degree of deformation or collapse. Notice from Figure 6 failure type the general shear failure in the soil below the foundation, where the concentration of stresses under the center of the foundation is shown in the color bar where the red color indicates the active region where the vertical stresses are at their maximum height and this corresponds to the direct influence region under the foundation as described by Terzaghi. As for the second region, the stresses decrease the further we move away from the center of footing and this corresponds to the radial region in Terzaghi's theory. The farther regions where the blue color indicates the resistance of the soil are passive regions for the stresses resulting from the load.

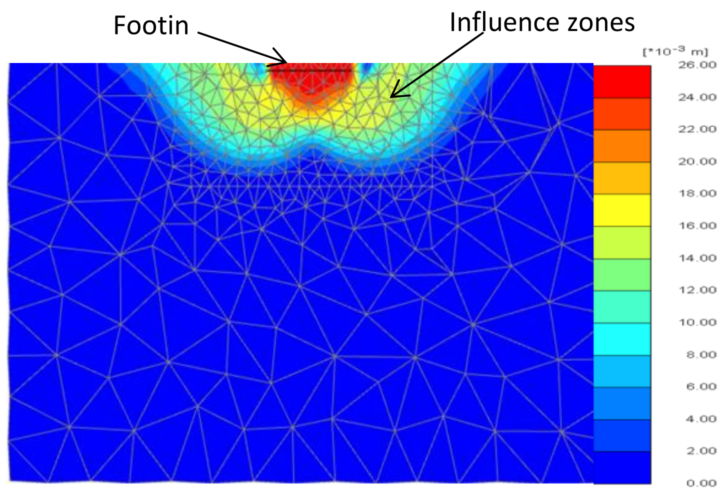

Fig. 6: General shear failure and Influence zones in clay soil of the Al-Habobi area finite element analysis using FE method.

In the other cases studied, the soil exhibited punching failure, a common occurrence in weak clay soils that lack sufficient strength to resist applied loads as shown in (Fig. 7), the finite elements were applied to the Karmashya area where the cohesion is equal to 24. Notice from the Figure that the type of failure that occurs in the soft clay soil is punching shear failure.

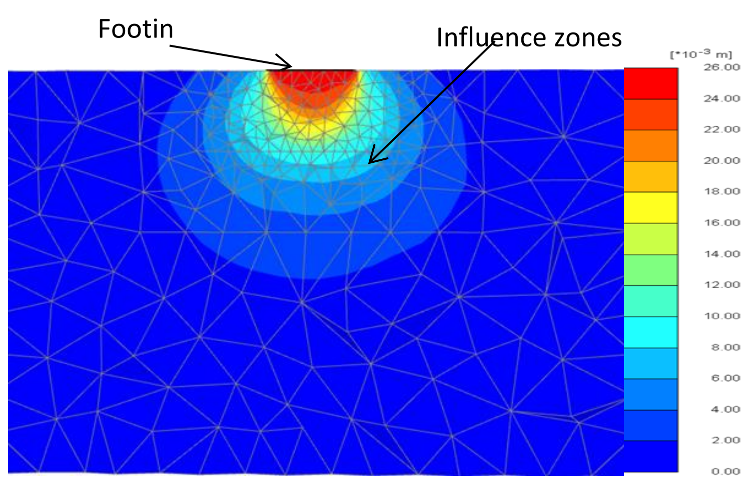

Fig. 7: Punching shear failure and influence zone in Clay Soil of the Karmashya area using FE analysis.

(Fig. 8) shows the difference in the boundaries of the failure zones according to Terzagi's theory and the finite element analysis using the Plaxis program according to the three failure zones proposed by Terzaghi. It is obvious that the boundary of failure surface is larger than failure zones boundary indicated by the finite element method.

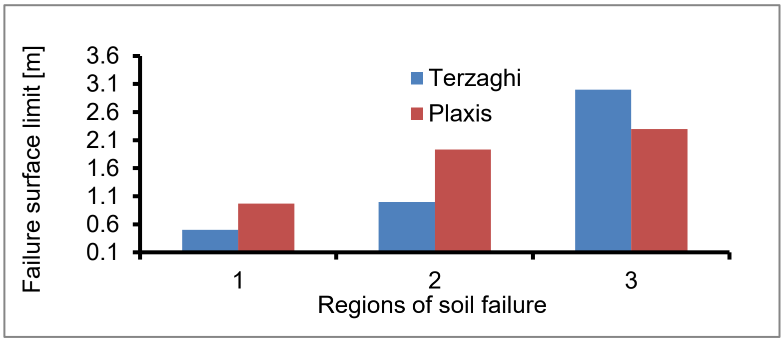

Fig. 8: Comparison of failure zones and limits of failure surfaces based on Terzaghi and Finite element solution.

5. Conclusion

Based on the analysis carried out using the finite element method and comparison with different theories to calculate the bearing capacity of clayey soils, the following conclusions can be outlined.

1) The finite element solution for the case of a square foundation on clay soil gave values of bearing capacity approximately similar to those obtained by Meyerhof's design equation, with the lowest error of 7%, which reflects high agreement. The results of bearing capacity computed by Hansen and Vesic equations compared with the finite element results showed an error rate of 8%, which indicates an acceptable agreement with the numerical results. In contrast, the results of the Prandtl and Terzaghi equations showed a higher error rate of 15%, which indicates that these models may be less accurate in predicting the behavior of clayey soils under the studied loads.

2) Related to the analysis of the results of the failure zone study, there is good agreement in the distribution of stresses in the soil under the foundation according to the numerical analysis with the other theoretical equations, but there is a difference in the limits of the failure surface. There is a difference in the values of the failure surface boundaries. According to Terzagh's theory the boundary of the influence zone was 1m to 3m, while for the numerical analysis, the values were 0.97m to 2.3m.

References

[1] A. B. AL-DAWOODI, F. H. RAHIL, and M. Q. WAHEED, "Numerical Simulation of Shallow Foundation Behavior Rested on Sandy Soil," *IOP Conf. Ser. Earth Environ. Sci.*, vol. 856, no. 1, 2021, doi: 10.1088/1755-1315/856/1/012042.

[2] J. K. DAS AND B. BHARALI, "A Simplified Numerical Approach to Predict Bearing Capacity of Soil for Shallow Foundation," *J. Appl. Eng. Sci.*, vol. 12, no. 1, pp. 33–36, 2022, doi: 10.2478/jaes-2022-0005.

[3] S. SRIHANDAYANI, A. HAKAM, M. MERA, and F. A. ISMAIL, "Bearing Capacity Analysis of Floating Foundation Model in Homogeneous Very Soft Clay," *Civ. Environ. Eng.*, vol. 19, no. 2, pp. 758–771, 2023, doi: 10.2478/cee-2023-0069.

[4] S. Van Baars, "100 Year Prandtl ' s Wedge - Intermediate report," pp. 1–109, 2016.

[5] K. TERZAGHI, *A fundamental fallacy in earth pressure computations*, no. 3. Harvard University, 1936.

[6] K. TERZAGHI, R. B. PECK, and G. MESRI, "Plastic equilibrium in soils," *Soil mechanics in engineering practice*. pp. 258–262, 1996.

[7] "KARL TERZAGHI," *Géotechnique*, vol. 13, no. 4, pp. 267–268, 1963, doi: 10.1680/geot.1963.13.4.267.

[8] G. G. MEYERHOF, "Some Recent Research on the Bearing Capacity of Foundations," *Can. Geotech. J.*, vol. 1, no. 1, pp. 16–26, 1963, doi: 10.1139/t63-003.

[9] A. S. VESIĆ, "Analysis of ultimate loads of shallow foundations," *J. soil Mech. Found. Div.*, vol. 99, no. 1, pp. 45–73, 1973.

[10] S. VAN BAARS, "The inclination and shape factors for the bearing capacity of footings," *Soils Found.*, vol. 54, no. 5, pp. 985–992, 2014, doi: 10.1016/j.sandf.2014.09.004.

[11] J. B. HANSEN, "A revised and extended formula for bearing capacity," 1970.

[12] M. Y. AL-AGHBARI and Y. E. A. MOHAMEDZEIN, "Bearing capacity of strip foundations with structural skirts," *Geotech. Geol. Eng.*, vol. 22, no. 1, pp. 43–57, 2004, doi:

10.1023/B:GEGE.0000013997.79473.e0.
[13] A. ALNMR and R. ALSIRAWAN, "Numerical Study of the Effect of the Shape and Area of Shallow Foundations on the Bearing Capacity of Sandy Soils," *Acta Polytech. Hungarica*, vol. 21, no. 1, pp. 103–120, 2024, doi: 10.12700/APH.21.1.2024.1.7.
[14] S. GUPTA AND A. MITAL, "Numerical analysis of bearing capacity of rectangular footing," *J. Phys. Conf. Ser.*, vol. 1240, no. 1, 2019, doi: 10.1088/1742-6596/1240/1/012039.
[15] R. A. FAHAD, R. R. SHAKIR, and H. M. ALI, "Evaluation on the SPT Based Design Approach for Shallow Foundations," *E3S Web Conf.*, vol. 427, pp. 1–10, 2023, doi: 10.1051/e3sconf/202342701025.
[16] A. A. ALTAWEEL and R. R. SHAKIR, "The Effect of Interference of Shallow Foundation on Settlement of Clay Soil," *IOP Conf. Ser. Mater. Sci. Eng.*, vol. 1094, no. 1, p. 012043, 2021, doi: 10.1088/1757-899x/1094/1/012043.
[17] Z. H. JAWAD and R. R. SHAKIR, "Behavior of Foundation Rested on Geogrid-Reinforced Soil : A Review," *IOP Conf. Ser. Mater. Sci. Eng.*, vol. 1094, no. 1, p. 012110, 2021, doi: 10.1088/1757-899x/1094/1/012110.
[18] A. A. ALTAWEEL and R. R. SHAKIR, "Analytical model for bearing capacity of two closely spaced foundations," *J. Phys. Conf. Ser.*, vol. 1973, no. 1, 2021, doi: 10.1088/1742-6596/1973/1/012199.
[19] R. SHAKIR, "Undrained Bearing Capacity for Strip Footing on Two Layered Elastic - Plastic Clay by Using FEM," *Eng. Technol. J.*, vol. 24, no. 6, pp. 651–669, 2005, doi: 10.30684/etj.24.6.4.
[20] R. L. MICHALOWSKI and L. SHI, "Bearing capacity of footings over two-layer foundation soils," *J. Geotech. Eng.*, vol. 121, no. 5, pp. 421–428, 1995.
[21] R. R. SHAKIR, "Spatial Correlation of Cone Tip Resistance for Soil in Nasiriyah," *Open Civ. Eng. J.*, vol. 12, no. 1, pp. 413–429, 2018, doi: 10.2174/1874149501812010413.
[22] 2006 J.C. GOF, and S.Z. JASSIM, "Geology of Iraq", Geological Society of London, "Initial settlement of structures on clay," *J. Soil Mech. Found. Div.*, vol. 97, no. 10, pp. 1359–1377, 1971.
[23] H. MOHAMMED ALI and R. R. SHAKIR, "Geotechnical map of Thi Qar governorate using geographical information systems (GIS)," *Mater. Today Proc.*, vol. 60, no. October, pp. 1286–1296, 2022, doi: 10.1016/j.matpr.2021.09.138.
[24] A. A. M. AQRAWI, "Correction of Holocene sedimentation rates for mechanical compaction: the Tigris-Euphrates Delta, Lower Mesopotamia," *Mar. Pet. Geol.*, vol. 12, no. 4, pp. 409–416, 1995, doi: 10.1016/0264-8172(95)96903-4.
[25] V. GALAVI and R. B. J. BRINKGREVE, "Finite element modelling of geotechnical structures subjected to moving loads," *Numer. Methods Geotech. Eng. - Proc. 8th Eur. Conf. Numer. Methods Geotech. Eng. NUMGE 2014*, vol. 1, no. July, pp. 235–240, 2014, doi: 10.1201/b17017-44.
[26] R. SHAKIR and R. R. SHAKIR, "Effect of an impervious core constructed into a large earth dam on the quantity of seepage Characterestic values of engineering properties in Nasseriya View project Effect of an impervious core constructed into a large earth dam on the quantity of seepage," no. January 2011, 2017, [Online]. Available: https://www.researchgate.net/publication/296705332
[27] R. R. SHAKIR and M. MAJEED, "Two Dimensional Consolidations for Clay Soil of Non-Homogeneous and Anisotropic Permeability," vol. 2, no. 10, pp. 4–9, 2014.
[28] J. DQG, W. K. H. KHDG, and D. W. DQ, "(VWLPDWLRQ WKH 4XDQWLW \ RI 6HHSDJH 8QGHU 6LQJOH," no. March 2004, 2021.
[29] A. THAKUR and R. KUMAR, "Experimental and numerical studies of skirted hexagonal footings on three sands," *SN Appl. Sci.*, vol. 2, no. 3, pp. 1–11, 2020, doi: 10.1007/s42452-020-2239-9.
[30] K. SIEN TI, B. B. HUAT, J. NOORZAEI, S. JAAFAR, and G. SEW CEO, "A review of basic soil constitutive models for geotechnical application," *Electron. J. Geotech. Eng.*, vol. 14, no. January 2009, pp. 1–18, 2009, [Online]. Available: https://www.researchgate.net/profile/Bujang-Huat/publication/228565882_A_Review_of_Basic_Soil_Constitutive_Models_for_Geotechnical_Application/links/598d5d2faca272e57ad3bcb6/A-Review-of-Basic-Soil-Constitutive-Models-for-Geotechnical-Application.pdf
[31] O. A. ARAB, A. J. M. S. LIM, S. Y. SIM, and N. A. A. GUNTOR, "Numerical Modelling Observations of Settlement for Pad Footings Supported on Soft Clay Soil," *IOP Conf. Ser. Mater. Sci. Eng.*, vol. 1200, no. 1, p. 012032, 2021, doi: 10.1088/1757-899x/1200/1/012032.
[32] S. VAN BAARS, "Failure mechanisms and corresponding shape factors of shallow foundations," in *Proceedings of 4th International Conference on New Developments in Soil Mechanics and Geotechnical Engineering*, Near East University Press, 2016.